ACS APPLIED MATERIALS & INTERFACES
Research Article
www.acsami.org

Nanointerlayer Induced Electroluminescence Transition from Ultraviolet- to Red-Dominant Mode for n-Mn:ZnO/N-GaN Heterojunction

Hai Zhou,[†] Guojia Fang,*[,†] Qike Jiang,[‡] Yongdan Zhu,[†] Nishuang Liu,[†] Xiao Zou,[†] Xiaoming Mo,[†] Yihe Liu,[†] Jianbo Wang,*[,‡] Xianquan Meng,[†] and Xingzhong Zhao[†]

[†]Department of Electronic Science and Technology and Key Laboratory of Artificial Micro- and Nano-structures of Ministry of Education, School of Physics and Technology, [‡]School of Physics and Technology Center for Electron Microscopy and MOE Key Laboratory of Artifcial Micro- and Nano-structures, Wuhan University, Wuhan 430072, People's Republic of China

Supporting Information

ABSTRACT: High-quality Mn:ZnO (MZO) film had been prepared on N-GaN coated sapphire substrates followed by postdeposition thermal annealing treatment at 700 °C. For the annealed MZO/GaN heterojunction, a 15 nm cubic structural $ZnGa_2O_4$ layer was observed at the MZO/GaN interface through transmission electron microscope analysis. Through electroluminescence (EL) measurement, the formation of the nanointerface results in an EL transition from ultraviolet- to red-dominant mode for n-Mn:ZnO/N-GaN heterojunction light-emitting diodes (LEDs). The heterojunction LED showed a rectification ratio of ~2.0×10^5 at ±2 V, a dark current of 3.5 nA at −2 V and a quite strong red EL with a low turn-on voltage of 3 V. On the basis of the energy band diagram, we think the EL transition from ultraviolet- to red-dominant mode is mainly due to the formation of a thin oxide blocking nanolayer at the MZO/GaN interface during the annealing process.

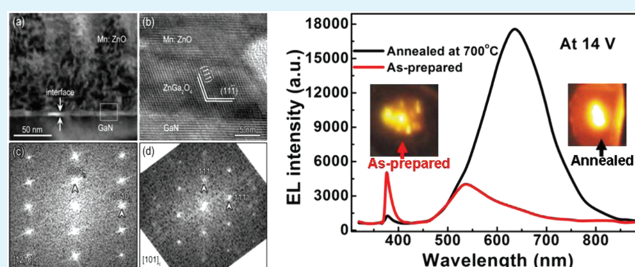

KEYWORDS: *red electroluminescence, Mn:ZnO, light-emitting diodes, low turn-on voltage, nano- interface, ultraviolet- to red-dominant*

1. INTRODUCTION

Recently, zinc oxide (ZnO) has attracted much attention for its applications in ultraviolet (UV) optoelectronic devices, such as UV light-emitting diodes (LEDs) and UV photodetectors (PDs), because of its wide band gap of ~3.3 eV and high transmittance (~ 90%) in the visible region.[1−6] As one of its doped compounds, Mn-doped ZnO (MZO) also shows very good optoelectronic characteristic.[7] MZO films have been prepared by many methods, such as metal−organic chemical vapor deposition (MOCVD),[8] magnetron sputtering[9] and sol gel.[10,11] Among these methods, the film prepared by conventional magnetron sputtering deposition is very economy and simple.

Red emission is an essential component for these practical applications in full-color displays and solid state lighting, together with green and blue emission. However, the reports about this red emission are seldom in ZnO-based devices. In our previous works, we have reported ZnO-based heterojunction LEDs with different structures,[12−15] all of which showed limited rectification ratios and very strong UV electroluminescence (EL) and quite weak EL in visible region.[12,13] And Li, et al.[14] reported n-ZnO/n-GaN Heterojunction LEDs, which showed a clear photovoltaic behavior with a power conversion efficiency of 0.57% and a violet emission peak centered at ~433 nm. Huang, et al.[15] reported an annealed n-ZnO/n-GaN structure and it showed a sharp UV emission centered at 367 nm and a broad orange emission centered at 640 nm under forward and reverse biases, respectively. Herein, we report a $Mn_{0.005}Zn_{0.995}O$/GaN heterojunction LED, which shows an EL transition from ultraviolet- to red-dominant mode at a forward bias when the heterojunction was thermal annealed at 700 °C for 2 h. Also the annealed heterojunction LED shows a rectification ratio of ~2.0×10^5 at ±2 V, a dark current of 3.5 nA at −2 V, and a quite strong red EL with a low turn-on voltage of 3 V. We think the reason is mainly due to the formation of a thin $ZnGa_2O_4$ layer at the MZO/GaN interface during the annealing process.

2. EXPERIMENTAL SECTION

The n-type undoped GaN-coated sapphire substrate was initially cleaned with acetone, ethanol, and deionized water, respectively, and then blown with dry N_2 before deposition. The n-GaN layer with a thickness of 3.2 μm has a resistivity and a carrier concentration of 9.13×10^{-2} Ω cm and 1.78×10^{17} cm^{-3}, respectively. Then, 80-nm MZO film was deposited on the GaN-coated sapphire substrate by radio frequency reactive magnetron sputtering at 100 °C. The films were deposited at total pressure of 2.0 Pa with a power of sputtering of 120

Received: February 9, 2012
Accepted: May 3, 2012
Published: May 3, 2012

 © 2012 American Chemical Society

W and an Ar/O_2 ratio of 8:3. Herein, the thickness of the MZO film is measured by a surface profilometer (Talysurf Serles II) and the MZO composition was determined by X-ray photoelectron spectroscopy (XPS). Before deposition, the target was presputtered for 10 min to remove some possible contaminants. Then, 80-nm-thick Au electrodes were patterned on the ZnO surface with a shadow mask by radio frequency reactive magnetron sputtering at room temperature. After that, the devices were annealed at 700 °C for 2 h in air. Finally, to get large-area Ohmic contacts to the surface of GaN, an In electrode was applied. The Au electrode area is $\pi \times 0.5^2$ mm^2 and the In electrode area is 1×0.5 mm^2. All the I−V characteristics were measured by a Keithley 4200 electrometer. The EL measurements were carried out in an Acton SpectroPro 2500 monochromator. Transmission electron microscope (TEM) techniques, including the bright field (BF) imaging, high resolution (HR) and the selected area electron diffraction (SAED), were performed using a JEOL JEM0−2010 (HT) electron microscope. All of these measurements were carried out at room temperature (RT) in ambient atmosphere.

3. RESULTS AND DISCUSSION

Figure 1a shows the TEM image of the n-MZO/N-GaN heterojunction annealed at 700 °C. Figure 1b illustrates the HR

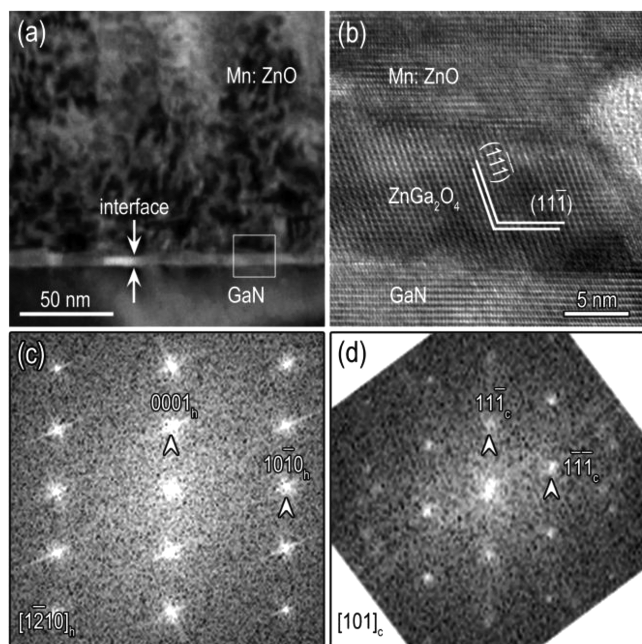

Figure 1. (a) TEM bright-field image of the Mn:ZnO/GaN heterojunction; (b) HRTEM image of the framed area in a; (c) Fast Fourier transform (FFT) pattern of the Mn:ZnO layer in b; (d) FFT pattern of the $ZnGa_2O_4$ layer in b. Subscripts "h" and "c" denote the hexagonal ZnO and cubic $ZnGa_2O_4$ phase, respectively.

TEM image of the white-framed area in Figure 1a, which reveals that an interfacial layer with a thickness of ~15 nm is formed during the thermal annealing process between MZO and GaN. Figure 1c and (d) show the Fast Fourier Transform (FFT) patterns of the MZO film and the interface, respectively, from which the interface is identified as a cubic $ZnGa_2O_4$ phase. The $ZnGa_2O_4$ nanofilm is formed between MZO and GaN by annealing at 700 °C in air, following a reaction equation

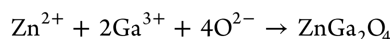

$$Zn^{2+} + 2Ga^{3+} + 4O^{2-} \rightarrow ZnGa_2O_4$$

In this work, the Zn^{2+} and Ga^{3+} comes from MZO and GaN, respectively, the O^{2-} comes from MZO or the air when the device is under high temperature. The orientation relationship between $ZnGa_2O_4$ and MZO can be determined to be $[101]_c//[1-210]_h$, $(11-1)_c//(0001)_h$. Subscripts "c" and "h" denote cubic $ZnGa_2O_4$ and hexagonal MZO phases, respectively. From the HR TEM image of the interface, we can see the crystal quality of the $ZnGa_2O_4$ film is very good. However, for the as-prepared n-MZO/N-GaN heterojunction, the interface is very vague (about 2 nm) and the crystal quality is not good, which can be seen in Figure 1 of the Supporting Information.

Figure 2 shows the RT PL spectra of GaN-coated sapphire substrate, *n*-MZO/*N*-GaN LEDs with and without postdeposition thermal annealing treatment. As shown in Figure 2, the GaN shows two peaks, the bigger one is located at ~361 nm, which is attributed to the band edge emission of GaN (3.4 eV), and the smaller one is at ~544 nm, which is due to the nitrogen vacancies or some threading dislocations in n-GaN. For the as-prepared device, it shows the same two peaks with that of GaN, but we can see the intensity of its UV emission is weaker than that of its visible emission, which may be due to the emission induced by the oxygen vacancies of MZO or Mn deep level defects. For the annealed device, it shows a different peak in UV region and the peak is at about 396 nm, which is attributed to Mn-doped ZnO film.

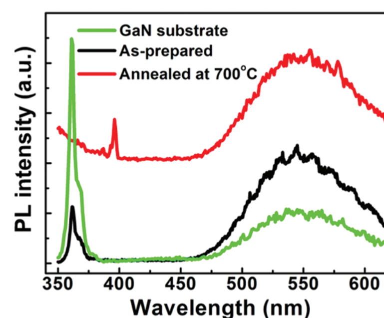

Figure 2. RT PL spectra of GaN-coated sapphire substrate, *n*-MZO/*N*-GaN LEDs with and without postdeposition thermal annealing treatment.

A schematic structure of *n*-MZO/*N*-GaN heterojunction diode in panels a and b in Figure 3 shows a typical current rectification from the *n*-MZO/*N*-GaN heterojunction. From this figure, at ±2 V, the as-prepared device shows a rectification ratio of ~32 and a dark current of 25 μA at −2 V bias. The reverse dark current is smaller than that of ZnO-based devices,[12,13] which may be due to Mn doping in ZnO. For the annealed devices, the rectification ratio reaches to ~2.0×10^5 when the annealing temperature is 700 °C. Also the device annealed at 700 °C shows a very low dark current of ~3.5 nA. The reason we think is due to the existence of the $ZnGa_2O_4$ and the improved quality of MZO film by annealing treatment. The $ZnGa_2O_4$ can limit the transmission of minority carriers as a blocking layer and the high-quality MZO film decreases the current induced by impurity scattering. These good diode characteristics will make our device work at a high voltage or current with little thermal effects and the reason we think is due to the formation of a thin $ZnGa_2O_4$ layer by the annealing treatment. The *I*−*V* curve of the annealed device exhibited a small current at 0 V, which may be attributed to the noise current in our test environment, also a little photocurrent induced by some visible light may be another reason. The inset shows the corresponding logarithmic *I*−*V* plots, where the ideality factor is deduced from the linear regime of the forward

dx.doi.org/10.1021/am300223y | ACS Appl. Mater. Interfaces 2012, 4, 2521−2524

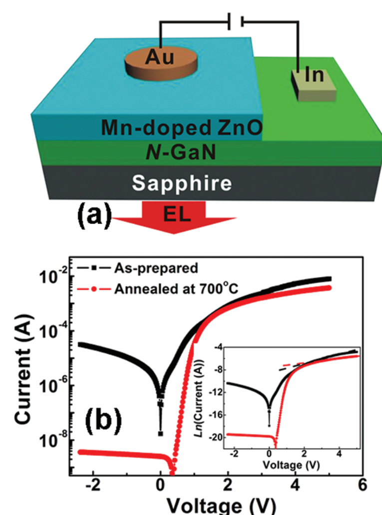

Figure 3. (a) Schematic diagram of the *n*-MZO/*N*-GaN structure on a sapphire substrate. (b) *I*−*V* curves of the *n*-MZO/*N*-GaN heterojunction LEDs. The inset shows the corresponding logarithmic *I*−*V* plots.

bias (tangential line). The ideality factor of the annealed device (∼2.4) is greater than that of as-prepared device (∼1.7), which suggests that the minority carrier transport of the annealed device is significantly dominated by carrier recombination.[16]

The RT EL spectra of the *n*-MZO/*N*-GaN heterojunction LEDs annealed at 700 °C have been observed and measured by an Acton SpectroPro 2500 monochromator with a 500 nm blaze grating with a scanning step size of 0.5 nm, and were shown in Figure 4. The insert shows the plot of EL intensity

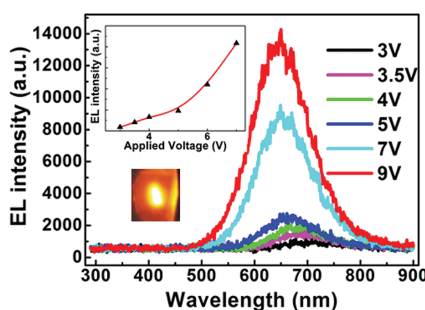

Figure 4. RT EL spectra of the annealed *n*-MZO/*N*-GaN heterojunction LEDs under different forward bias. The inset shows the plot of EL intensity versus forward bias fixing the emission wavelength at 650 nm (left up) and the lighting image (left down).

versus forward bias fixing the emission wavelength at 650 nm (left up) and the lighting image (left down). We can see that the EL spectra of LEDs are mainly in red region and the spectra exhibit peaks centered at 700, 691, 681, 666, 653, and 646 nm with the forward biases of 3.0, 3.5, 4.0, 5.0, 7.0, and 9.0 V, respectively. Also, we can see there are no UV emissions from our device when the forward bias increases from 3.0 to 9.0 V. From above, we can conclude that the red emission is dominant at a low bias. From the insert of Figure 4 (left up), the emission intensity enhances very much when the applied voltage increases and the turn-on voltage of the LEDs is 3 V, which is comparable to that of ZnO-based LEDs.[12,13]

The RT EL spectra of *n*-MZO/*N*-GaN LEDs measured at 14 V with and without postdeposition thermal annealing treatment are shown in Figure 5 and the measurement background is the same. The insert of Figure 5 shows the lighting image of the as-

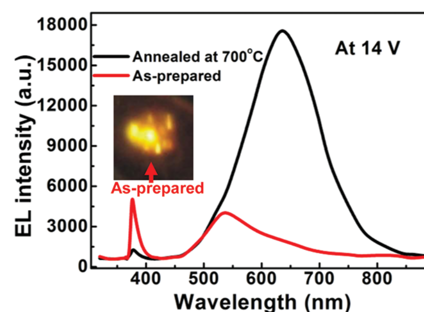

Figure 5. RT EL spectra of the *n*-MZO/*N*-GaN heterojunction LEDs at 14 V. The inset shows the lighting image of the as-prepared sample.

prepared sample. From this figure, we can see the *n*-MZO/*N*-GaN LED without annealing shows a relatively strong UV emission at the wavelength of 376 nm and a weak visible emission, but the annealed device shows an opposite behavior: a strong red emission accompanied by a weak UV emission. Furthermore, at a low applied voltage there is no UV emission for the annealed device, which can be seen in Figure 4. For the as-prepared *n*-MZO/*N*-GaN LED heterojunction LEDs, the UV emission located at 376 nm, is mainly attributed to the band-edge emission of ZnO (3.3 eV) and the visible emission of the as-prepared device is around 544 nm, which corresponds to the PL emission shown in Figure 2. For the annealed device, the peak of the visible emission shows a huge red-shift and is located at about 644 nm. The reason of the red-shift we will discuss later. From above, we can find that the EL characteristic shows a transition from UV- to red-dominant mode when the device is annealed. From Figure 2 and 5, it should be noted that there are some differences between PL and EL emission. One reason is attributed to the difference between PL and EL processes: the EL is collected through the GaN/Sapphire substrate, while PL is collected from MZO side surface.[17] The other is that the EL emission probably occurs near the interfacial layer, whereas the PL emission is mainly taken place at the surface of MZO.[15]

From above, there are significant characteristic differences between the as-prepared and the annealed devices. For the as-prepared *n*-MZO/*N*-GaN heterojunction LED, there is not an effectively blocking layer at the MZO/*N*-GaN interface and the electrons from GaN side can easily enter into MZO film. So the UV emission of the as-prepared device may origin from the band edge of ZnO and the weak visible emission around 544 nm may come from the defects of the MZO or GaN. For the annealed *n*-MZO/*N*-GaN heterojunction, the red emission is related to the high quality oxide nanolayer, $ZnGa_2O_4$, formed at the MZO/GaN interface. Under a high electric field, most of the voltage will be applied on the $ZnGa_2O_4$ layer for its dielectric nature and the holes are generated in this i-$ZnGa_2O_4$ layer by the high-electric-field-induced impact ionization.[13] Under a forward bias, the electrons in GaN can be efficiently injected into the $ZnGa_2O_4$ interface layer, which may result in the recombination of electron−hole pairs and the red emission. The UV emission of the annealed device appears at a high voltage, the reason we think is that: at a low bias, the recombination of electron−hole pairs in the $ZnGa_2O_4$ interface layer will be preferred, so the device shows a wide red EL. When the applied voltage increases and reaches to a high value,

such as 14 V, the energy bands will be further bended. Electrons from GaN may tunnel through the thin $ZnGa_2O_4$ interface layer to get MZO side, and/or the holes induced by impact ionization may tunnel through the thin interface layer to get GaN side, a weak band edge emission of GaN or ZnO appears. Therefore, the annealed MZO/GaN heterojunction LED shows a red-dominant mode.

■ CONCLUSION

In conclusion, a 15 nm cubic structural $ZnGa_2O_4$ layer was formed at the MZO/GaN interface when the MZO/GaN heterojunction was annealed at 700 °C. For n-Mn:ZnO/N-GaN heterojunction LEDs, the formation of the nanointerface resulting in a transition of EL from ultraviolet- to red-dominant mode. The heterojunction LED showed a rectification ratio of $\sim 2.0 \times 10^5$ at ± 2 V, a dark current of 3.5 nA. Also the annealed heterojunction LEDs display a strong red electroluminescence with a low turn-on voltage of 3 V. The reason we think is mainly due to the formation of a metal oxide blocking nanolayer at the MZO/GaN interface during the annealing process.

■ ASSOCIATED CONTENT

Supporting Information

TEM images of the as-prepared Mn:ZnO/GaN heterojunction are available as Supporting Information. This material is available free of charge via the Internet at http://pubs.acs.org.

■ AUTHOR INFORMATION

Corresponding Author

*E-mail: gjfang@whu.edu.cn (G.F.); wang@whu.edu.cn (J.W.).

Notes

The authors declare no competing financial interest.

■ ACKNOWLEDGMENTS

This work was partially supported by the Natural Science Foundation of China (11074194), the National Basic Research Program (2011CB933300) of China, the Research Program of Suzhou Science & Technology Bureau (SYG201133), and by the Natural Science Foundation of Hubei province (2010CDA016) and the Fundamental Research Funds for the Central Universities.

■ REFERENCES

(1) Liu, C. H.; Zapien, J. A.; Yao, Y.; Meng, X. M.; Lee, C. S.; Fan, S. S.; Lifshitz, Y.; Lee, S. T. *Adv. Mater.* **2003**, *15*, 838−841.

(2) Kind, H.; Yan, H.; Messer, B.; Law, M.; Yang, P. *Adv. Mater.* **2002**, *14*, 158−160.

(3) Soci, C.; Zhang, A.; Xiang, B.; Dayeh, S. A.; Aplin, D. P. R.; Park, J.; Bao, X. Y.; Lo, Y. H.; Wang, D. *Nano Lett.* **2007**, *7*, 1003−1009.

(4) Li, Q. H.; Gao, T.; Wang, Y. G.; Wang, T. H. *Appl. Phys. Lett.* **2005**, *86*, 123117.

(5) Harnack, O.; Pacholski, C.; Weller, H.; Yasuda, A.; Wessels, J. M. *Nano Lett.* **2003**, *3*, 1097−1101.

(6) Zhou, H.; Fang, G.; Yuan, L.; Wang, C.; Yang, X.; Huang, H.; Zhou, C.; Zhao, X. *Appl. Phys. Lett.* **2009**, *94*, 013503.

(7) Wu, Y.; Rao, K. V.; Voit, W.; Tamaki, T.; Jayakumar, O. D.; Belova, L.; Liu, Y. S.; Glans, P. A.; Chang, C. L.; Guo, J. *IEEE Trans. Magn.* **2010**, *46*, 2152−2155.

(8) Chikoidze, E.; Dumont, Y.; Von Bardeleben, H. J.; Gleize, J.; Jomard, F.; Rzepka, E.; Berrerar, G.; Ferrand, D.; Gorochov, O. *Appl. Phys. A: Mater. Sci. Process.* **2007**, *88*, 167−171.

(9) Yadav, H. K.; Sreenivas, K.; Gupta, V. *J. Appl. Phys.* **2006**, *99*, 083507.

(10) Wang, J.; Chen, W.; Wang, M. *J. Alloys Compd.* **2008**, *449*, 44−47.

(11) Deepa, M.; Bahadur, N.; Srivastava, A. K.; Chaganti, P.; Sood, K. N. *J. Phys. Chem. Solids* **2009**, *70*, 291−297.

(12) Long, H.; Fang, G.; Li, S.; Mo, X.; Wang, H.; Huang, H.; Jiang, Q.; Wang, J.; Zhao, X. *IEEE Electron. Device Lett.* **2011**, *32*, 54−56.

(13) Li, S.; Fang, G.; Long, H.; Mo, X.; Huang, H.; Dong, B.; Zhao, X. *Appl. Phys. Lett.* **2010**, *96*, 201111.

(14) Li, S.; Fang, G.; Long, H.; Wang, H.; Huang, H.; Mo, X.; Zhao, X. *IEEE Photonics Technol. Lett.* **2012**, *24*, 137−139.

(15) Huang, H.; Fang, G.; Li, S.; Long, H.; Mo, X.; Wang, H.; Li, Y.; Jiang, Q.; Carroll, D. L.; Wang, J.; Wang, M.; Zhao, X. *Appl. Phys. Lett.* **2011**, *99*, 263502.

(16) Jung, Y.; Vacic, A.; Perea, D. E.; Picraux, S. T.; Reed, M. A. *Adv. Mater.* **2011**, *23*, 4306−4311.

(17) Zhang, S. G.; Zhang, X. W.; Yin, Z. G.; Wang, J. X.; Dong, J. J.; Wang, Z. G.; Qu, S.; Cui, B.; Wowchak, A. M.; Dabiran, A. M.; Chow, P. P. *J. Appl. Phys.* **2011**, *109*, 093708.